

Modeling the adiabatic connection in H₂

Michael J. G. Peach, Andrew M. Teale,^{a)} and David J. Tozer^{b)}

Department of Chemistry, University of Durham, South Road, Durham DH1 3 LE, United Kingdom

(Received 26 March 2007; accepted 14 May 2007; published online 22 June 2007)

Full configuration interaction (FCI) data are used to quantify the accuracy of approximate adiabatic connection (AC) forms in describing the ground state potential energy curve of H₂, within spin-restricted density functional theory (DFT). For each internuclear separation R , accurate properties of the AC are determined from large basis set FCI calculations. The parameters in the approximate AC form are then determined so as to reproduce these FCI values exactly, yielding an exchange-correlation energy expressed entirely in terms of FCI-derived quantities. This is combined with other FCI-derived energy components to give the total electronic energy; comparison with the FCI energy quantifies the accuracy of the AC form. Initial calculations focus on a [1/1]-Padé-based form. The potential energy curve determined using the procedure is a notable improvement over those from existing DFT functionals. The accuracy near equilibrium is quantified by calculating the bond length and vibrational wave numbers; errors in the latter are below 0.5%. The molecule dissociates correctly, which can be traced to the use of virtual orbital eigenvalues in the slope in the noninteracting limit, capturing static correlation. At intermediate R , the potential energy curve exhibits an unphysical barrier, similar to that noted previously using the random phase approximation. Alternative forms of the AC are also considered, paying attention to size extensivity and the behavior in the strong-interaction limit; none provide an accurate potential energy curve for all R , although good accuracy can be achieved near equilibrium. The study demonstrates how data from correlated *ab initio* calculations can provide valuable information about AC forms and highlight areas where further theoretical progress is required. © 2007 American Institute of Physics. [DOI: 10.1063/1.2747248]

I. INTRODUCTION

The success of Kohn-Sham density functional theory^{1,2} (DFT) relies on the accurate representation of the exchange-correlation energy E_{XC} . Significant insight into this quantity is obtained from the adiabatic connection (AC),³⁻¹⁰ which considers a series of N -electron systems with Hamiltonians

$$\hat{H}_\lambda = \hat{T} + \lambda \hat{V}_{ee} + \sum_i v_\lambda(\mathbf{r}_i), \quad (1)$$

where \hat{T} is the electronic kinetic energy operator and λ is a coupling strength parameter that scales the electron-electron interaction, $\hat{V}_{ee} = \sum_{i < j} 1/r_{ij}$. The final term is the external potential, which is varied so as to keep the density fixed at its physical value.⁵ The AC smoothly connects the Kohn-Sham noninteracting system ($\lambda=0$) to the interacting physical system ($\lambda=1$) and, through the Hellmann-Feynman theorem, provides an exact expression for the exchange-correlation energy,

$$E_{XC} = \int_0^1 d\lambda W_\lambda, \quad (2)$$

where

^{a)}Permanent address: Department of Chemistry, University of Oslo, PO Box 1033, Blindern, N-0315 Oslo, Norway.

^{b)}Fax: 0191 384 4737. Electronic mail: dj.tozer@Durham.ac.uk

$$W_\lambda = \langle \Psi_\lambda | \sum_{i < j} \frac{1}{r_{ij}} | \Psi_\lambda \rangle - J. \quad (3)$$

Here, Ψ_λ is the ground state wave function of the system with Hamiltonian \hat{H}_λ , and J is the Coulomb energy,

$$J = \frac{1}{2} \iint d\mathbf{r}_1 d\mathbf{r}_2 \frac{\rho(\mathbf{r}_1)\rho(\mathbf{r}_2)}{r_{12}}, \quad (4)$$

where $\rho(\mathbf{r})$ is the electron density. When $\lambda=0$, the wave function is the noninteracting Kohn-Sham single determinant Ψ_0 , so

$$W_0 = \langle \Psi_0 | \sum_{i < j} \frac{1}{r_{ij}} | \Psi_0 \rangle - J = E_X, \quad (5)$$

where E_X is the exact orbital exchange energy, defined as in Hartree-Fock theory but evaluated using Kohn-Sham orbitals. When $\lambda=1$, the wave function is the exact wave function of the interacting physical system, Ψ_1 , so

$$W_1 = \langle \Psi_1 | \sum_{i < j} \frac{1}{r_{ij}} | \Psi_1 \rangle - J = V_{ee} - J, \quad (6)$$

which is the difference between the total electron-electron repulsion energy V_{ee} of the interacting physical system and the Coulomb energy. It follows that the correlation kinetic energy, defined by $T_C = E_{XC} - (V_{ee} - J)$, is given by

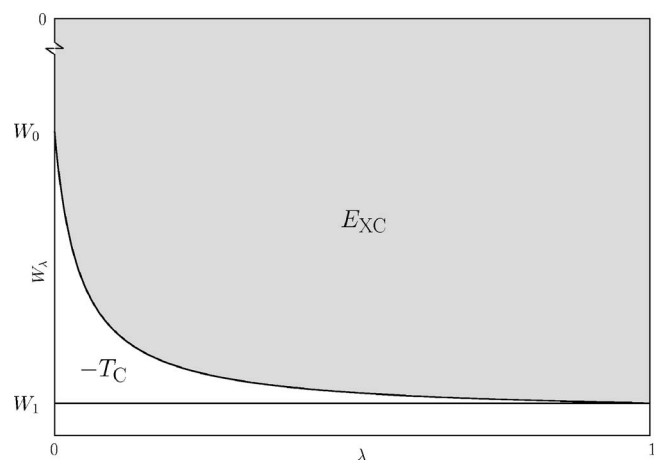


FIG. 1. Schematic representation of the adiabatic connection. E_{XC} and $-T_C$ are given by the integrals, as indicated.

$$T_C = E_{XC} - W_1. \quad (7)$$

As illustrated in Fig. 1, E_{XC} and T_C have a simple geometrical interpretation in terms of the AC. The exact slope of W_λ at $\lambda=0$ is twice the second-order correlation energy from Görling-Levy density functional perturbation theory^{11,12} (GL2),

$$\left. \frac{\partial W_\lambda}{\partial \lambda} \right|_{\lambda=0} = 2E_C^{GL2} = -\frac{1}{2} \sum_{ij\alpha\beta} \frac{[(\alpha i|\beta j) - (\alpha j|\beta i)]^2}{\varepsilon_\alpha + \varepsilon_\beta - \varepsilon_i - \varepsilon_j} - 2 \sum_{i\alpha} \frac{\langle \varphi_i | v_X - v_X^{NL} | \varphi_\alpha \rangle^2}{\varepsilon_\alpha - \varepsilon_i}. \quad (8)$$

Here, the first term is twice the conventional second-order Møller-Plesset energy expression, involving two-electron integrals of occupied (i, j) and virtual (α, β) Kohn-Sham orbitals and their associated eigenvalues ε . The second term involves the difference between the multiplicative exchange potential v_X and the nonmultiplicative (nonlocal, NL) exchange, v_X^{NL} .

There have been a number of attempts to develop exchange-correlation functionals by explicitly approximating W_λ and evaluating the energy using Eq. (2). Examples include the half-and-half functional of Becke¹³ [the precursor of the Becke-3-Lee-Yang-Parr functional¹⁴⁻¹⁷ (B3LYP)]; the [1/1]-Padé-based form of Ernzerhof,¹⁸ the two-legged representation of Burke *et al.*;¹⁹ and the interaction strength interpolation of Seidl *et al.*²⁰ Mori-Sánchez, Cohen, and Yang²¹ (MCY) recently proposed two functionals based on the same form considered by Ernzerhof,¹⁸

$$W_\lambda^{MCY} = a + \frac{b\lambda}{1 + c\lambda}, \quad (9)$$

but with alternative definitions of the three parameters.

The quantities a and b in Eq. (9) define the value and slope, respectively, of W_λ^{MCY} at $\lambda=0$. To satisfy Eq. (5), Mori-Sánchez *et al.* defined the parameter a to be the exchange energy E_X . In order to avoid the computational expense of the GL2 slope evaluation, they defined b as a modified Tao-Perdew-Staroverov-Scuseria²² (TPSS) slope, with an additional scaling factor of 4.0 to optimize thermochemi-

cal performance. The parameter c was chosen such that W_λ^{MCY} equalled the BLYP (Ref. 16 and 23) value at $\lambda=0.63$, again to optimize performance. This functional was denoted as MCY1. A second functional (denoted as MCY2) involving an additional scaling factor was introduced to improve atomic energies. A key feature of the MCY functionals is that they are one-electron self-interaction-free, meaning that the exchange-correlation energy exactly cancels the Coulomb energy for any one-electron density; this follows because, as defined, $b=0$ for a one-electron system and so the exchange-correlation energy reduces to the exchange energy, as required. They are not, however, many electron self-interaction-free.^{24,25} The performance of the functionals is encouraging, notably providing a simultaneously good description of thermochemistry and kinetics.²¹

The quality of the MCY functionals is governed by the mathematical form of Eq. (9) and the procedure used to determine the three parameters. An obvious (but necessary) deficiency is that although the leading parameter was determined so as to reproduce a known property of the exact AC, the other two were not. The first aim of the present study is to use correlated *ab initio* calculations to investigate the performance of the W_λ form in Eq. (9) when all three parameters are determined so as to reproduce accurate properties of the AC—this will establish how well the exact AC can be represented using this form. As the test, we shall consider the singlet ground state potential energy curve of the H_2 molecule, which is the famous and challenging example of static electron correlation. The small size of this system allows essentially exact *ab initio* calculations to be performed and the two-electron nature affords several welcome simplifications. The work is particularly relevant in light of the recent study by Fuchs *et al.*,²⁶ who considered H_2 dissociation using the random phase approximation (RPA);^{3,5} see Ref. 26 for a detailed discussion of H_2 dissociation in DFT. The second aim of the study is to extend the analysis to other AC forms, paying attention to size extensivity and the behavior in the strong-interaction limit.

We commence in Sec. II by describing how large basis set full configuration interaction (FCI) calculations can be used to determine accurate properties of the AC. In Sec. III, the three parameters in the AC form in Eq. (9) are determined so as to reproduce these FCI values exactly, yielding an exchange-correlation energy expressed entirely in terms of FCI-derived quantities. This is then combined with other FCI-derived energy components to give the total electronic energy. The H_2 potential energy curve and related properties determined in this manner are compared with conventional DFT results and FCI reference values, allowing the accuracy of the AC form to be quantified. The analysis is extended to other AC forms in Sec. IV. Conclusions are presented in Sec. V.

II. COMPUTATIONAL DETAILS

All calculations in this study use the CADPAC program,²⁷ with the extensive aug-cc-pV6Z orbital basis set,²⁸ omitting g and h functions for technical reasons. The H_2 molecule is treated in its singlet ground state using the appropriate spin-

restricted formalism throughout—no unrestricted calculations are performed. The FCI calculations provide exact results within the extensive basis set; the dissociation energy agrees with that of Kolas and Wolniewicz²⁹ to within 0.1%.

Our first task is to calculate accurate properties of the AC. In principle, an accurate AC curve can be determined by evaluating Eq. (3) using wave functions from FCI calculations, and although this is nontrivial for arbitrary λ , it is straightforward when λ is 0 or 1. For $\lambda=0$, evaluation of Eq. (5) using FCI data gives the exchange energy, determined using the Kohn-Sham orbitals associated with the FCI density. For a two-electron system, the exchange energy is minus one-half of the Coulomb energy, and so

$$W_0^{\text{FCI}} = -\frac{1}{2}J^{\text{FCI}}, \quad (10)$$

where J^{FCI} is the Coulomb energy in Eq. (4), evaluated using the FCI density. For $\lambda=1$, evaluation of Eq. (6) using the FCI data gives

$$W_1^{\text{FCI}} = V_{\text{ee}}^{\text{FCI}} - J^{\text{FCI}}, \quad (11)$$

where $V_{\text{ee}}^{\text{FCI}}$ is the FCI electron-electron repulsion energy, obtained by subtracting the nuclear-nuclear repulsion and one-electron energies (determined using the FCI density matrix) from the FCI total electronic energy. Eqs. (10) and (11) represent exact values of the AC, within the basis set, which can easily be determined from a FCI calculation.

The slope at $\lambda=0$ is twice the GL2 energy, given in Eq. (8), evaluated using the Kohn-Sham orbitals and eigenvalues associated with the FCI density. For this two-electron system, v_X in the second term of Eq. (8) is minus one-half of the Coulomb potential, since the potential is the functional derivative of the corresponding energy. Given that there is only one occupied orbital φ_1 , it follows that

$$\langle \varphi_1 | v_X | \varphi_\alpha \rangle = \langle \varphi_1 | v_X^{\text{NL}} | \varphi_\alpha \rangle, \quad (12)$$

for all virtual orbitals φ_α . Hence the latter term in Eq. (8) is identically zero and

$$\left. \frac{\partial W_\lambda^{\text{FCI}}}{\partial \lambda} \right|_{\lambda=0} = -\frac{1}{2} \sum_{ij\alpha\beta} \frac{[(\alpha i | \beta j) - (\alpha j | \beta i)]^2}{\varepsilon_\alpha + \varepsilon_\beta - \varepsilon_i - \varepsilon_j}. \quad (13)$$

Evaluation of this expression requires the Kohn-Sham orbitals and eigenvalues associated with the FCI density and the accuracy of these quantities will depend on the method used to obtain them. We use the Wu-Yang³⁰ (WY) implementation of the constrained search formulation,^{31,32} which minimizes the noninteracting kinetic energy subject to the constraint that the FCI density is recovered. A well-balanced description of the orbitals and potential is known to be important^{33,34} in the closely related Yang-Wu optimized effective potential scheme³⁵ and so we use the same (truncated) aug-cc-pV6Z basis set²⁸ for the expansion of both the orbitals and potential. We use a Fermi-Amaldi³⁶ reference potential, which provides essentially identical results to those obtained using a Slater reference potential.³⁷ We use a cutoff of 1×10^{-6} in the truncated singular value decomposition, which provides essentially identical results to those obtained using a cutoff of 1×10^{-8} . Further reduction in the cutoff is

numerically undesirable. By construction, the density from the Kohn-Sham occupied orbital should equal the FCI density and so the accuracy of the calculations can be judged by comparing the Coulomb energies [Eq. (4)] from the two densities. For the range of H_2 internuclear separations (R) considered ($0.7 \text{ bohr} \leq R \leq 10 \text{ bohrs}$), the energies from the two densities differ by a maximum of 5×10^{-6} hartree ($7 \times 10^{-4} \%$).

Schipper *et al.*³⁸ have demonstrated that the exchange-correlation potential that exactly corresponds to a finite Gaussian basis set density can exhibit unphysical, oscillatory structure. The exchange-correlation potentials in our WY calculations do exhibit minor undulations when R is large. In order to obtain a smooth, more physically sensible potential, we have performed additional calculations using the procedure of Heaton-Burgess *et al.*,³⁴ which introduces a smoothing norm into the minimization. The potentials do become very smooth but, importantly, the potential energy curves (see later) are essentially indistinguishable from those obtained without the smoothing norm. The FCI density is less well reproduced, however, because the procedure limits the extent to which the solution point ($\rho = \rho^{\text{FCI}}$) can be reached.

For a two-electron system, the exchange-correlation potential that yields the finite basis FCI density can be determined exactly from a direct inversion of the Kohn-Sham equation;³⁹ see Ref. 40 for a related study on the H_2 molecule. We have performed a direct inversion and—consistent with Schipper *et al.*³⁸—find that the potential is oscillatory in the vicinity of the nuclei. A third way to determine orbitals and eigenvalues is therefore to solve the finite basis set Kohn-Sham problem with this potential. Again, the potential energy curves are virtually indistinguishable from those above, although the FCI density is reproduced less well, this time due to the use of a finite basis set. Throughout this study, Eq. (13) is therefore evaluated using the first of the three described procedures.

Evaluation of Eqs. (10), (11), and (13) provides accurate AC data for H_2 . In Secs. III and IV, these data will be used to determine the parameters in approximate AC forms such that these FCI values, or some subset of them, are reproduced exactly. The associated exchange-correlation energies will then be determined entirely in terms of FCI-derived quantities and so any error in the exchange-correlation energy can be attributed to the failure of the approximate AC form to reproduce the exact AC. In practical calculations, it is more convenient to deal with total electronic energies and their related properties, rather than exchange-correlation energies. The nuclear-electron and Coulomb components of the total energy are always explicit functionals of the density, so can be calculated exactly, within the basis set, by evaluating them using the FCI density. For two-electron systems, the occupied Kohn-Sham orbital is the square root of one-half of the electron density, and so the noninteracting kinetic energy, which is generally a functional of the orbitals, also becomes an explicit functional of the density. Specifically, it is given by the von Weizsäcker expression,⁴¹

$$T_s = T_W = \frac{1}{8} \int d\mathbf{r} \frac{|\nabla\rho(\mathbf{r})|^2}{\rho(\mathbf{r})}, \quad (14)$$

and so this component can also be evaluated exactly from the FCI density. The only other component is the nuclear-nuclear repulsion, which is trivial to determine. We therefore define our total DFT electronic energy for H_2 as

$$E = T_W^{\text{FCI}} + E_{\text{ne}}^{\text{FCI}} + J^{\text{FCI}} + E_{\text{nn}} + E_{\text{XC}}, \quad (15)$$

where T_W^{FCI} and $E_{\text{ne}}^{\text{FCI}}$ are the von Weizsäcker and nuclear-electron energies, respectively, evaluated using the FCI density. The first four terms are exact and the error in the final term arises entirely from the approximate AC form. Comparison of energies from Eq. (15) with those from FCI will therefore allow the accuracy of the AC form to be quantified.

III. APPLICATION TO THE W_λ^{MCY} FORM

As a first application, we consider the AC form in Eq. (9). We introduce the notation

$$W_\lambda^{\text{ACI}} = a + \frac{b\lambda}{1+c\lambda} \quad (16)$$

for which the exchange-correlation energy in Eq. (15) is²¹

$$E_{\text{XC}}^{\text{ACI}} = a + \frac{b}{c} \left(1 - \frac{\log_e(1+c)}{c} \right). \quad (17)$$

We define the parameters a , b , and c , by requiring that the value and slope of W_λ^{ACI} at $\lambda=0$, together with the value at $\lambda=1$, equal the FCI values of Sec. II,

$$W_0^{\text{ACI}} = a = W_0^{\text{FCI}}, \quad (18)$$

$$\left. \frac{\partial W_\lambda^{\text{ACI}}}{\partial \lambda} \right|_{\lambda=0} = b = \left. \frac{\partial W_\lambda^{\text{FCI}}}{\partial \lambda} \right|_{\lambda=0}, \quad (19)$$

and

$$W_1^{\text{ACI}} = a + \frac{b}{1+c} = W_1^{\text{FCI}}. \quad (20)$$

From Eqs. (10), (11), and (13), it follows that

$$a = -\frac{1}{2} J^{\text{FCI}}, \quad (21)$$

$$b = -\frac{1}{2} \sum_{ij\alpha\beta} \frac{[(\alpha i|\beta j) - (\alpha j|\beta i)]^2}{\epsilon_\alpha + \epsilon_\beta - \epsilon_i - \epsilon_j}, \quad (22)$$

using Kohn-Sham quantities from the WY calculation, and

$$c = \frac{b}{V_{\text{ee}}^{\text{FCI}} - J^{\text{FCI}} - a} - 1. \quad (23)$$

For each H_2 internuclear separation, an FCI calculation was performed and the quantities a , b , and c in Eqs. (21)–(23), were determined. These were used to evaluate the exchange-correlation energy using Eq. (17), which was then combined with the other FCI-derived components in Eq. (15), to determine the total electronic energy. Results from this procedure are denoted as ACI.

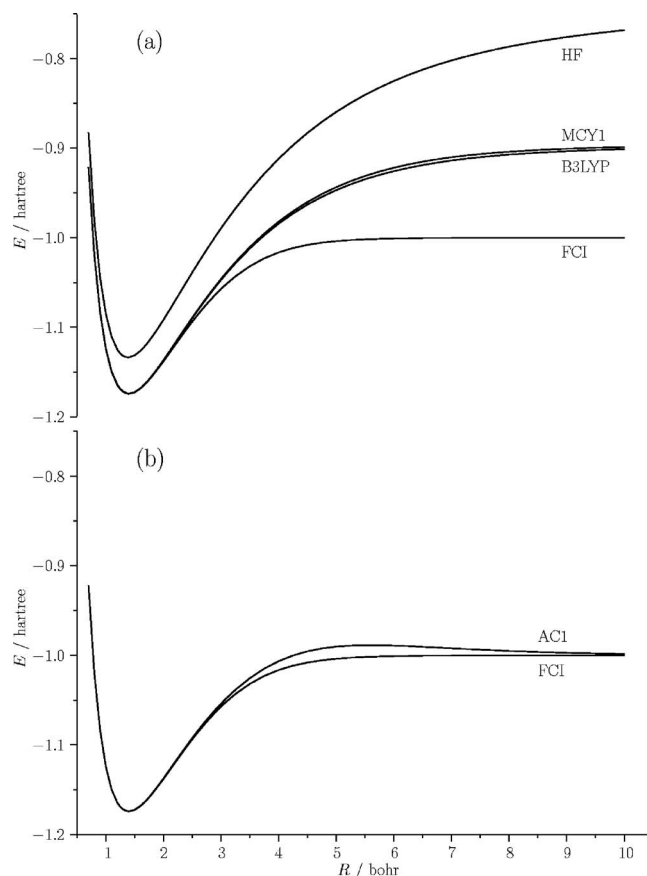


FIG. 2. Potential energy curve of H_2 determined using FCI, compared with those from (a) HF, MCY1, and B3LYP; and (b) ACI.

We first consider potential energy curves of H_2 determined using standard methods, reiterating that all calculations in this study use the appropriate spin-restricted formalism. Figure 2(a) compares self-consistent Hartree-Fock (HF) and B3LYP curves with the FCI reference curve. HF is very poor, reflecting the 50% unphysical ionic contribution ($H^+ \cdots H^-$) to the wave function at dissociation. The B3LYP curve is an improvement, but significant error remains. Also shown is the self-consistent MCY1 curve, which is similar to the MCY2 curve (not shown). MCY1 provides similar performance to B3LYP while removing the one-electron self-interaction error.

Figure 2(b) compares the ACI potential energy curve with the FCI reference curve. It is a significant improvement over those of Fig. 2(a). We stress that the improvement is not simply a consequence of using improved Kohn-Sham orbitals; we have performed MCY1 calculations using the WY orbitals and the shape of the potential energy curve barely changes from the MCY1 curve in Fig. 2(a), other than by an upward shift due to the non variational nature of such calculations.

ACI provides a good description of the potential energy curve in the region of the minimum. MCY1 and B3LYP are also accurate in this region, while HF is poor. To quantify the accuracy, Table I presents optimized bond lengths R_e for the methods, comparing with the FCI value, which agrees with experiment to the precision quoted. All three DFT methods give bond lengths to within 0.001 bohr of FCI; the bond

TABLE I. Bond lengths (R_e) in bohr, and zero-point (ZP), fundamental ($v=0 \rightarrow v=1$), and first overtone ($v=0 \rightarrow v=2$) vibrational wave numbers in cm^{-1} , compared to experimental values.

	HF	B3LYP	MCY1	AC1	FCI	Expt.
R_e	1.386	1.402	1.401	1.400	1.401	1.401 ^a
ZP	2274	2186	2191	2185	2180	2179 ^b
$v=0 \rightarrow v=1$	4373	4188	4197	4176	4162	4161 ^b
$v=0 \rightarrow v=2$	8546	8163	8182	8121	8088	8087 ^b

^aReference 42.^bDetermined using the Dunham coefficients in Ref. 42, with the Kaiser correction (Ref. 43).

length is notably underestimated with HF. The potential energy curves have also been used to determine vibrational energy levels, using the LEVEL 7.5 code of Le Roy.⁴⁴ The potential energy curves used as input consisted of points in the range of $0.7 \text{ bohr} \leq R \leq 3.5 \text{ bohrs}$, with a spacing of 0.01 bohr ; we have confirmed that the quoted results are converged with respect to these quantities. Convergence of the calculated levels was set to $1 \times 10^{-2} \text{ cm}^{-1}$ and ten-point piecewise polynomial interpolation was used. Zero-point, fundamental, and overtone wave numbers ($J=0$) are presented in Table I, comparing with the FCI values, which agree with experiment to within 1 cm^{-1} . AC1 provides the best agreement with FCI, with errors of 5, 14, and 33 cm^{-1} , respectively for zero point, fundamental, and overtone; the corresponding percentage errors are 0.2%, 0.3%, and 0.4%. The next best results are obtained with B3LYP, where the errors are 6, 26, and 75 cm^{-1} . MCY1 errors are 11, 35, and 94 cm^{-1} . All three functionals therefore provide a good quality zero-point wave number, but the differences between the methods become more pronounced for the higher levels, with MCY1 and (to a lesser extent) B3LYP degrading. The HF errors are significantly larger.

Figure 2(b) further demonstrates that at large R , AC1 also provides results in excellent agreement with FCI—static correlation is recovered. In fact, the dissociation limit is obtained exactly because as $R \rightarrow \infty$, the quantity $b \rightarrow -\infty$, due to the eigenvalue degeneracy in the denominator of Eq. (22). It follows that the exchange-correlation energy in Eq. (17) approaches the value W_1^{AC1} , which, by construction, equals W_1^{FCI} in Eq. (11). Given that there is no electron-electron repulsion, this is just the negative of the FCI coulomb energy, and so the exchange-correlation energy exactly cancels the Coulomb one and the total energy in Eq. (15) reduces to the sum of the one-electron contributions, as required. This is also evident from a consideration of the derivative of Eq. (16),

$$\frac{\partial W_\lambda^{\text{AC1}}}{\partial \lambda} = \frac{b}{(1 + c\lambda)^2}, \quad (24)$$

as $R \rightarrow \infty$, which exhibits the correct behavior, as described in Ref. 26. When $\lambda=0$, the gradient equals b , which is minus infinity in the limit. For any nonzero λ , however, the gradient is zero due to the quadratic divergence in the denominator. As $R \rightarrow \infty$, the quantity W_λ^{AC1} therefore drops from its value of $W_0^{\text{AC1}}=a$ with an infinite slope, acquiring the constant value $W_1^{\text{AC1}}=2a$ for all nonzero λ , thereby trivially integrating to an energy of W_1^{AC1} . It follows that T_C is exactly zero (recall Fig. 1), which is appropriate in this case as it com-

prises two isolated one-electron systems. The reader is referred to Fig. 2 of Ref. 26 and the discussion of Fig. 3, below. It is worth noting that this lack of λ dependence in W_λ^{AC1} (i.e., $T_C=0$) will occur whenever $b \rightarrow -\infty$, for example, in the dissociation of a general homonuclear diatomic molecule. In cases with many electron fragments, it will be in-

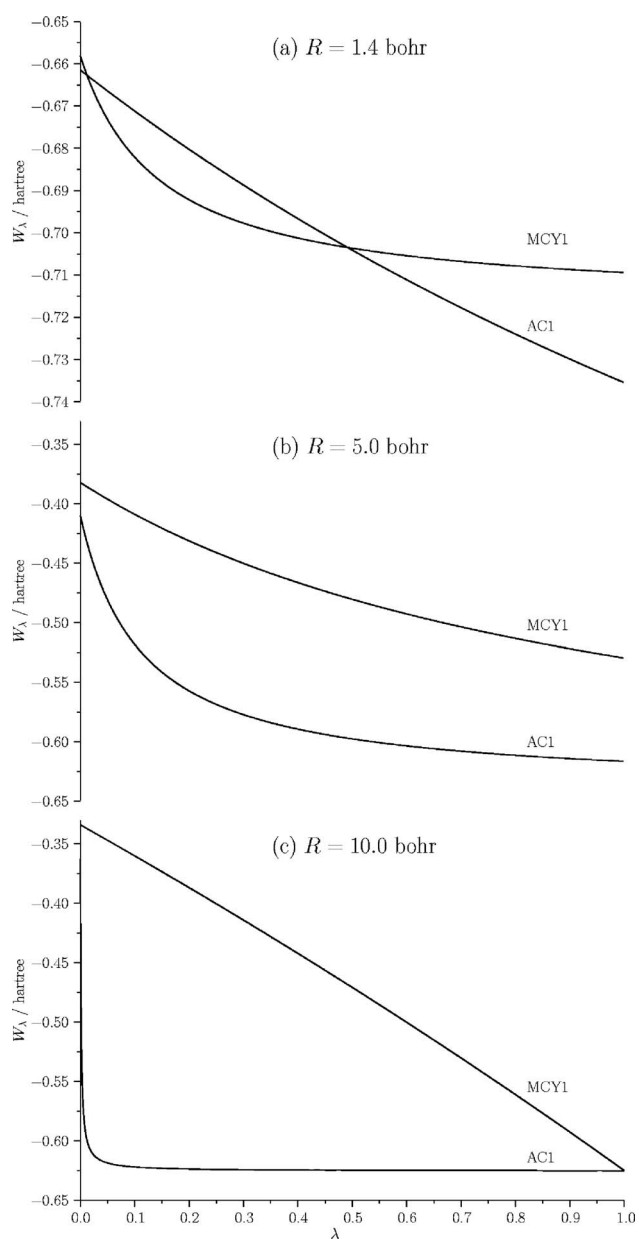
FIG. 3. Comparison of W_λ from AC1 and MCY1, evaluated at internuclear separations of (a) 1.4 bohr (equilibrium), (b) 5 bohrs; and (c) 10 bohrs.

TABLE II. Exchange-correlation energies, in hartrees, calculated using FCI and AC1, as functions of internuclear separation R , in bohrs. Also presented are the AC1 percentage errors.

R	E_{XC}^{FCI}	E_{XC}^{AC1}	% Error
1.0	-0.7857	-0.7857	0.0
1.4	-0.7024	-0.7023	0.0
2.0	-0.6174	-0.6169	0.1
3.0	-0.5543	-0.5510	0.6
4.0	-0.5642	-0.5543	1.8
5.0	-0.5941	-0.5805	2.3
6.0	-0.6118	-0.6001	1.9
7.0	-0.6196	-0.6115	1.3
8.0	-0.6228	-0.6178	0.8
9.0	-0.6241	-0.6212	0.5
10.0	-0.6246	-0.6230	0.3

correct to have $T_C=0$. Mori-Sánchez *et al.*²¹ cite the related example of the uniform electron gas.

Next, consider intermediate regions in Fig. 2(b). The AC1 curve resembles that obtained by Fuchs *et al.*,²⁶ using the RPA. There is an unphysical barrier, which is the first significant discrepancy compared to FCI. We reiterate that this feature is unaffected by smoothing the potential in the WY procedure or the use of the direct inversion alternative. This does not imply, however, that it is insensitive to the choice of orbitals and eigenvalues in Eq. (22). Replacing the FCI-based WY quantities with those from the Perdew-Burke-Ernzerhof⁴⁵ functional more than doubles the size of the barrier; using Hartree-Fock quantities causes a further significant increase. See Ref. 46 for a discussion of the orbital dependence of this feature in the RPA. We interpret the barrier in Fig. 2(b) as a failure of Eq. (16). Consistent with this, we note that Fuchs *et al.*²⁶ used a similar form to represent their near-exact AC near equilibrium, but had to introduce additional flexibility into the form at intermediate R .

Table II quantifies the AC1 error in Fig. 2(b). Rather than presenting total electronic energies, only the exchange-correlation component is presented; the error is the same. The values may provide a useful reference for future studies of exchange-correlation in H_2 . The first column lists exact values determined from FCI,

$$E_{XC}^{FCI} = E^{FCI} - T_W^{FCI} - E_{ne}^{FCI} - J^{FCI} - E_{nn}, \quad (25)$$

where E^{FCI} is the FCI total electronic energy. The second column lists AC1 energies and the third column lists the associated percentage errors. The error at the equilibrium geometry (1.4 bohr) is 10^{-4} hartree, which represents the AC1 error in the dissociation energy. The maximum discrepancy occurs at 5 bohrs, where the energy difference is 1.35×10^{-2} hartree (2.3%). This error is about one-half of that obtained with the RPA in the study of Fuchs *et al.*²⁶

It is instructive to examine the shape of W_λ^{AC1} in the three cases. Figure 3 presents W_λ^{AC1} plots at (a) $R=1.4$ bohr, (b) 5.0 bohrs, and (c) 10.0 bohrs. The self-consistent MCY1 curves are presented for comparison. Both methods define W_0 to equal the exchange energy, but the values are different in practice because the MCY1 calculations use the self-

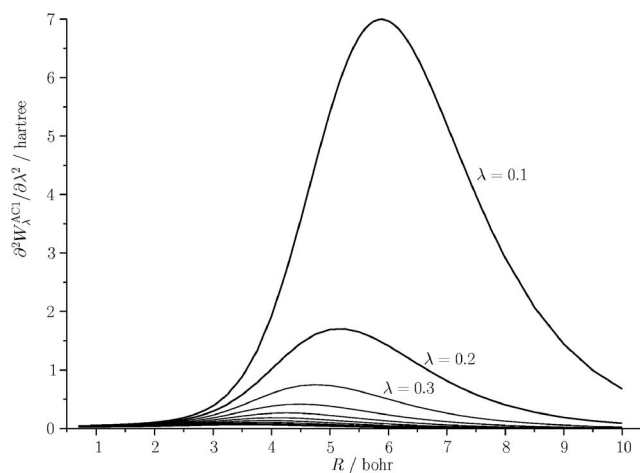


FIG. 4. $\partial^2 W_\lambda^{AC1} / \partial \lambda^2$, as a function of R for various values of λ .

consistent MCY1 exchange energy, whereas AC1 uses Eq. (21). At the equilibrium bond length ($R=1.4$ bohr), the two curves have a different shape, but the integrals, which determine E_{XC} through Eq. (2), are similar; the potential energy curves are therefore similar near equilibrium. The AC1 curve in Fig. 3(a) closely resembles the “exact” curve of Fuchs *et al.*²⁶ As R increases [Figs. 3(b) and 3(c)], the MCY1 integral becomes significantly less negative than that of AC1 and this is again reflected in the potential energy curves. At $R=10$ bohrs, the AC1 curve is almost flat; it will become completely flat, as discussed above, as $R \rightarrow \infty$. Interestingly, for this internuclear separation the MCY1 and AC1 curves have very similar values at $\lambda=1$ and so the failure of MCY1 can be attributed almost entirely to the incorrect slope at $\lambda=0$. The modified TPSS slope used in MCY1 does not diverge; the slope actually becomes less negative with increasing R . The GL2 slope used in AC1 does diverge, due to its dependence on the virtual orbital eigenvalues—static correlation is recovered. As with the potential energy curve, we have confirmed that the MCY1 curves in Fig. 3 do not improve when they are evaluated using the WY orbitals.

Figure 4 presents $\partial^2 W_\lambda^{AC1} / \partial \lambda^2$, plotted as a function of R , for a range of λ values. The curve for $\lambda=0$ is not presented due to the divergence at large R . For all the λ values shown, the curvature is small near equilibrium, increases to a maximum for intermediate R , then decreases again near dissociation. The observation that the associated potential energy curve is accurate at equilibrium and dissociation, but relatively poor in the intermediate regions, indicates that the form in Eq. (16) works well when the curvature is limited, but less well when it is higher. Inclusion of higher order terms in the expansion appears desirable, but would require additional input data. The high curvature of W_λ and the associated failure of Eq. (16) at intermediate R may reflect the fact that the nature of the exact wave function changes very rapidly in this region of the potential energy curve,⁴⁷ as evidenced by rapid changes in the occupation numbers of the σ_g and σ_u natural orbitals.

IV. APPLICATION TO OTHER W_λ FORMS

Calculations using the exchange-correlation energy in Eq. (17), with parameters a , b , and c defined as in Sec. III or

Ref. 21, are not in general size extensive.^{48,49} The energy of a system composed of two-noninteracting closed-shell fragments A and B does not equal the sum of the energies of the two fragments when A and B are different, although it does when they are the same. We complete this study by considering polynomial AC forms, which provide size-extensive models. We continue to define W_λ in terms of parameters a , b , and c , but their definitions may differ from those in Sec. III. We first consider the two forms

$$W_\lambda^{\text{AC2}} = a + b\lambda, \quad (26)$$

$$W_\lambda^{\text{AC3}} = a + b\lambda + c\lambda^2,$$

for which the exchange-correlation energies are

$$E_{\text{XC}}^{\text{AC2}} = a + \frac{b}{2}, \quad (27)$$

$$E_{\text{XC}}^{\text{AC3}} = a + \frac{b}{2} + \frac{c}{3}.$$

For AC2, we can require that the value and slope of W_λ^{AC2} at $\lambda=0$ equal the FCI values of Sec. II,

$$W_0^{\text{AC2}} = a = W_0^{\text{FCI}}, \quad (28)$$

$$\left. \frac{\partial W_\lambda^{\text{AC2}}}{\partial \lambda} \right|_{\lambda=0} = b = \left. \frac{\partial W_\lambda^{\text{FCI}}}{\partial \lambda} \right|_{\lambda=0} \quad (29)$$

and so a and b are evaluated using Eqs. (21) and (22). The potential energy curve determined in this manner is denoted as AC2 in Fig. 5(a). It is in poor agreement with FCI near equilibrium, diverging as R increases, due to the divergence of b . In light of the half-and-half (H&H) work of Becke,¹³ who also used the AC2 linear interpolation, we can alternatively require that the values of W_λ^{AC2} equal the FCI values at $\lambda=0$ and $\lambda=1$; this can be regarded as an exact representation of the half-and-half functional. In this case, Eq. (29) is replaced by

$$W_1^{\text{AC2}} = a + b = W_1^{\text{FCI}}, \quad (30)$$

and so from Eq. (11),

$$b = V_{\text{ee}}^{\text{FCI}} - J^{\text{FCI}} - a. \quad (31)$$

The curve determined in this manner is denoted as AC2(H&H) in Fig. 5(b). It is again in poor agreement with FCI near equilibrium but there is no divergence at large R , as the GL2 energy is not used.

AC3 contains three parameters and so, as in Sec. III, we require that the value and slope of W_λ^{AC3} at $\lambda=0$, together with the value at $\lambda=1$, equal the FCI values. It follows that a and b are evaluated using Eqs. (21) and (22) while c is determined from

$$W_1^{\text{AC3}} = a + b + c = W_1^{\text{FCI}}, \quad (32)$$

and so from Eq. (11),

$$c = V_{\text{ee}}^{\text{FCI}} - J^{\text{FCI}} - a - b, \quad (33)$$

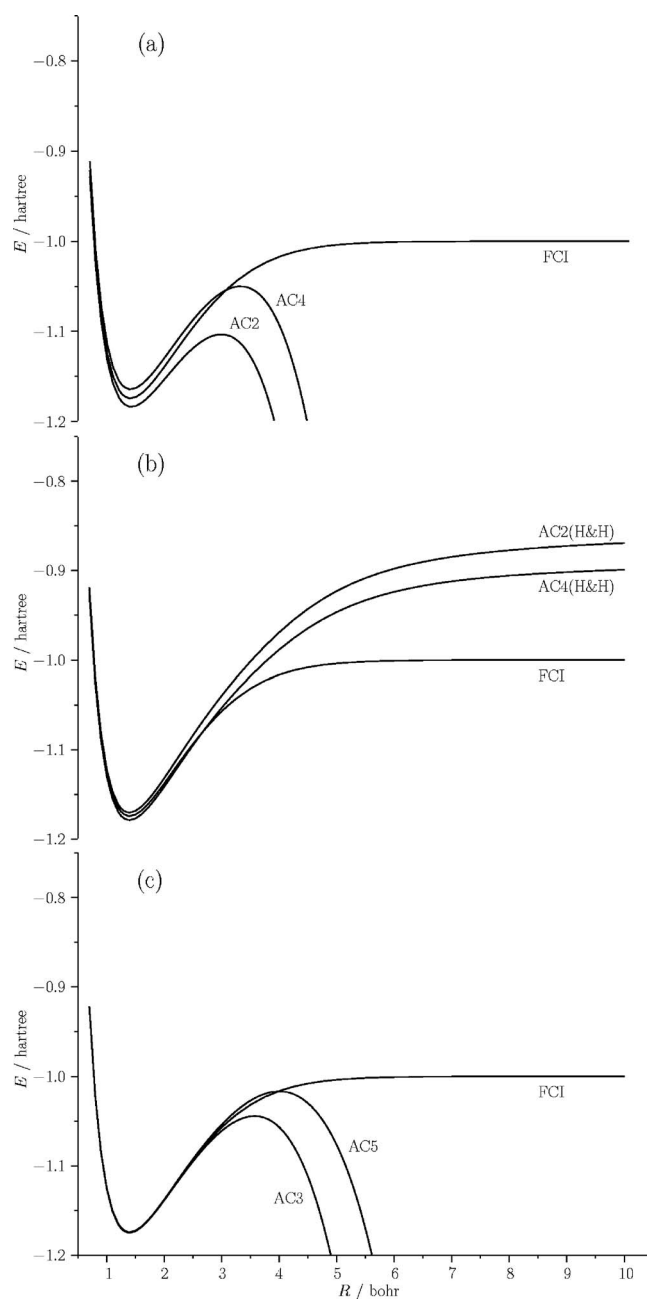


FIG. 5. Potential energy curve of H_2 determined using FCI, compared with those from size-extensive models. See text for details.

The potential energy curve determined in this manner is denoted as AC3 in Fig. 5(c). The agreement with FCI near equilibrium is now much improved. The minimum energy is at 1.402 bohr and the zero-point, fundamental, and overtone vibrational wave numbers are underestimated by just 4, 9, and 20 cm^{-1} , which are the smallest errors obtained in this study. The curve again diverges with increasing R , albeit more slowly than with AC2. The inclusion of higher order terms in λ would again appear desirable.

The forms in Eq. (26) give energies that are size extensive and one-electron self-interaction-free (when b and c are defined as above and a is evaluated as the exchange energy); however, they do not scale to a constant in the strong-interaction ($\lambda \rightarrow \infty$) limit⁵⁰ when b and c are nonzero. This leads us to consider the alternative forms

$$W_{\lambda}^{\text{AC4}} = a + b \left(\frac{\lambda}{1 + \lambda} \right),$$

$$W_{\lambda}^{\text{AC5}} = a + b \left(\frac{\lambda}{1 + \lambda} \right) + c \left(\frac{\lambda}{1 + \lambda} \right)^2,$$
(34)

which do scale to a constant when b and c are finite; the corresponding energies are

$$E_{\text{XC}}^{\text{AC4}} = a + b(1 - \log_e(2)),$$

$$E_{\text{XC}}^{\text{AC5}} = a + b(1 - \log_e(2)) + c(3/2 - 2 \log_e(2)).$$
(35)

Using exactly the same approach as for AC2 and AC3 (but with amended definitions of b and c where appropriate), we have determined potential energy curves using the AC forms in Eq. (34). The results are denoted as AC4, AC4(H&H), and AC5 and are presented in Figs. 5(a)–5(c), respectively. Compared to the AC2, AC2(H&H), and AC3 curves, the behavior at large R is improved; the AC5 curvature is higher than that of AC3, leading to an overestimation in the vibrational wave numbers.

V. CONCLUSION

We have used FCI data to quantify the accuracy of approximate AC forms in describing the ground state potential energy curve of H_2 within spin-restricted DFT, which is the famous and challenging example of static electron correlation. The key idea is to calculate accurate properties of the AC using FCI-derived data and then determine the parameters in approximate AC forms so as to reproduce these values exactly. The FCI density is also used to calculate the non-exchange-correlation components of the total electronic energy, allowing the accuracy of the various AC forms to be quantified.

Initially, we focused on the AC in Eq. (16), which has been considered previously by Ernzerhof¹⁸ and Mori-Sánchez *et al.*²¹ A particularly attractive feature of this form is that an appropriate choice of b can easily eliminate one-electron self-interaction.²¹ The potential energy curve determined using our approach is a significant improvement over those from Hartree-Fock and existing DFT functionals. The accuracy near equilibrium has been quantified by evaluating the bond length and vibrational wave numbers; errors in the latter are below 0.5%. The molecule dissociates correctly, which can be traced to the use of the GL2 slope. As in Refs. 26, 51, and 52, the present study therefore highlights the importance of virtual orbitals and eigenvalues for capturing static electron correlation effects. At intermediate R , the potential energy curve exhibits an unphysical barrier, which resembles that observed in Ref. 26 using the random phase approximation, but the magnitude in the present study is about half the size. Analysis of the curvature of the AC indicates that Eq. (16) works well when there is limited curvature, but less well when it is higher. The high curvature and failure of Eq. (16) at intermediate R may reflect the rapidly changing nature of the exact wave function in this region of the potential energy curve.

We have subsequently considered AC representations that lead to size-extensive models. Neither a straightforward linear nor quadratic polynomial can provide an accurate potential energy curve for all R , although the quadratic form is accurate near equilibrium. We have also considered two alternative forms that can scale correctly to a constant in the strong-interaction limit, which lead to improvements at large R .

Notwithstanding the high computational cost, the study demonstrates how data from correlated *ab initio* calculations can provide valuable information about AC forms and highlight areas where further theoretical progress is required, most notably in the description of the slope in the noninteracting limit.

ACKNOWLEDGMENTS

The authors are grateful to A. J. Cohen and W. Yang for providing the code for calculating MCY1 potential energy curves and AC curves and for providing a preprint of Ref. 34. They thank T. Helgaker, E. Tellgren, R. J. Bartlett, A. Görling, and T. Gimon for helpful discussions. Support from the EPSRC and the Norwegian Research Council (Grant No. 171185) is gratefully acknowledged.

- ¹ P. Hohenberg and W. Kohn, Phys. Rev. **136**, B864 (1964).
- ² W. Kohn and L. J. Sham, Phys. Rev. **140**, A1133 (1965).
- ³ D. C. Langreth and J. P. Perdew, Solid State Commun. **17**, 1425 (1975).
- ⁴ O. Gunnarsson and B. I. Lundqvist, Phys. Rev. B **13**, 4274 (1976).
- ⁵ D. C. Langreth and J. P. Perdew, Phys. Rev. B **15**, 2884 (1977).
- ⁶ J. P. Perdew, M. Ernzerhof, and K. Burke, J. Chem. Phys. **105**, 9982 (1996).
- ⁷ M. Levy, Phys. Rev. A **43**, 4637 (1991).
- ⁸ D. P. Joubert and G. P. Srivastava, J. Chem. Phys. **109**, 5212 (1998).
- ⁹ F. Colonna and A. Savin, J. Chem. Phys. **110**, 2828 (1999).
- ¹⁰ D. Frydel, W. M. Terilla, and K. Burke, J. Chem. Phys. **112**, 5292 (2000).
- ¹¹ A. Görling and M. Levy, Phys. Rev. B **47**, 13105 (1993).
- ¹² A. Görling and M. Levy, Phys. Rev. A **50**, 196 (1994).
- ¹³ A. D. Becke, J. Chem. Phys. **98**, 1372 (1993).
- ¹⁴ A. D. Becke, J. Chem. Phys. **98**, 5648 (1993).
- ¹⁵ P. J. Stephens, F. J. Devlin, C. F. Chabalowski, and M. J. Frisch, J. Phys. Chem. **98**, 11623 (1994).
- ¹⁶ C. Lee, W. Yang, and R. G. Parr, Phys. Rev. B **37**, 785 (1988).
- ¹⁷ S. H. Vosko, L. Wilk, and M. Nusair, Can. J. Phys. **58**, 1200 (1980).
- ¹⁸ M. Ernzerhof, Chem. Phys. Lett. **263**, 499 (1996).
- ¹⁹ K. Burke, M. Ernzerhof, and J. P. Perdew, Chem. Phys. Lett. **265**, 115 (1997).
- ²⁰ M. Seidl, J. P. Perdew, and S. Kurth, Phys. Rev. Lett. **84**, 5070 (2000).
- ²¹ P. Mori-Sánchez, A. J. Cohen, and W. Yang, J. Chem. Phys. **124**, 091102 (2006).
- ²² J. Tao, J. P. Perdew, V. N. Staroverov, and G. E. Scuseria, Phys. Rev. Lett. **91**, 146401 (2003).
- ²³ A. D. Becke, Phys. Rev. A **38**, 3098 (1988).
- ²⁴ P. Mori-Sánchez, A. J. Cohen, and W. Yang, J. Chem. Phys. **125**, 201102 (2006).
- ²⁵ A. Ruzsinszky, J. P. Perdew, G. I. Csonka, O. A. Vydrov, and G. E. Scuseria, J. Chem. Phys. **126**, 104102 (2007).
- ²⁶ M. Fuchs, Y.-M. Niquet, X. Gonze, and K. Burke, J. Chem. Phys. **122**, 094116 (2005).
- ²⁷ R. D. Amos, I. L. Alberts, J. S. Andrews *et al.*, CADPAC6.5, The Cambridge Analytic Derivatives Package, Cambridge, England, 1998.
- ²⁸ K. A. Peterson, D. E. Woon, and T. H. Dunning, Jr., (unpublished).
- ²⁹ W. Kołos and L. Wolniewicz, J. Chem. Phys. **43**, 2429 (1965).
- ³⁰ Q. Wu and W. Yang, J. Chem. Phys. **118**, 2498 (2003).
- ³¹ M. Levy, Proc. Natl. Acad. Sci. U.S.A. **76**, 6062 (1979).
- ³² M. Levy, Phys. Rev. A **26**, 1200 (1982).
- ³³ A. M. Teale, A. J. Cohen, and D. J. Tozer, J. Chem. Phys. **126**, 074101 (2007).
- ³⁴ T. Heaton-Burgess, F. A. Bulat, and W. Yang, arXiv:cond-mat/0610884.

- ³⁵W. Yang and Q. Wu, Phys. Rev. Lett. **89**, 143002 (2002).
- ³⁶E. Fermi and E. Amaldi, Accad. Ital. Rome **6**, 117 (1934).
- ³⁷J. C. Slater, Phys. Rev. **81**, 385 (1951).
- ³⁸P. R. T. Schipper, O. V. Gritsenko, and E. J. Baerends, Theor. Chem. Acc. **98**, 16 (1997).
- ³⁹C. J. Umrigar and X. Gonze, Phys. Rev. A **50**, 3827 (1994).
- ⁴⁰M. A. Buijse, E. J. Baerends, and J. G. Snijders, Phys. Rev. A **40**, 4190 (1989).
- ⁴¹C. F. von Weizsäcker, Z. Phys. **96**, 431 (1935).
- ⁴²K. P. Huber and G. Herzberg, *Molecular Spectra and Molecular Structure: Constants of Diatomic Molecules* (Van Nostrand, New York, 1979), Vol. 4.
- ⁴³E. W. Kaiser, J. Chem. Phys. **53**, 1686 (1970).
- ⁴⁴R. J. Le Roy, LEVEL 7.5, A computer program for solving the radial schrödinger equation for bound and quasibound levels, 2002, see the "Computer Programs" link at <http://leroy.uwaterloo.ca>
- ⁴⁵J. P. Perdew, K. Burke, and M. Ernzerhof, Phys. Rev. Lett. **77**, 3865 (1996).
- ⁴⁶N. E. Dahlen, R. van Leeuwen, and U. von Barth, Phys. Rev. A **73**, 012511 (2006).
- ⁴⁷N. C. Handy (private communication).
- ⁴⁸R. J. Bartlett and G. D. Purvis, Int. J. Quantum Chem. **14**, 561 (1978).
- ⁴⁹T. Helgaker, P. Jørgensen, and J. Olsen, *Molecular Electronic-Structure Theory* (Wiley, New York, 2000).
- ⁵⁰M. Levy and J. P. Perdew, Phys. Rev. A **32**, 2010 (1985).
- ⁵¹E. J. Baerends, Phys. Rev. Lett. **87**, 133004 (2001).
- ⁵²M. Grüning, O. V. Gritsenko, and E. J. Baerends, J. Chem. Phys. **118**, 7183 (2003).